

Effects of Orbital Eccentricity on Extrasolar Planet Transit Detectability and Light Curves

JASON W. BARNES

NASA Ames Research Center, Moffett Field, CA; jason@barnesos.net

Received 2007 July 9; accepted 2007 August 1; published 2007 September 12

ABSTRACT. It is shown herein that planets with eccentric orbits are more likely to transit than circularly orbiting planets with the same semimajor axis by a factor of $(1 - e^2)^{-1}$. If the orbital parameters of discovered transiting planets are known, as from follow-up radial velocity observations, then the transit-detected planet population is easily debiased of this effect. The duration of a planet's transit depends on its eccentricity and longitude of periastron; transits near periastron are shorter, and those near apoastron last longer, for a given impact parameter. If fitting for the stellar radius with the other transit parameters, this effect causes a systematic error in the resulting measurements. If the stellar radius is instead held fixed at a value measured independently, then it is possible to place a lower limit on the planet's eccentricity using photometry alone. Orbital accelerations cause a difference in the planet's ingress and egress durations that lead to an asymmetry in the transit light curve that could be used along with the transit velocity measurement to uniquely measure the planet's eccentricity and longitude of periapsis. However, the effect is too small to be measured with current technology. The habitability of transiting terrestrial planets found by *Kepler* depends on those planets' orbital eccentricities. While *Kepler* will be able to place lower limits on those planets' orbital eccentricity, the actual value for any given planet will likely remain unknown.

1. INTRODUCTION

There are presently 21 extrasolar planets known to transit their parent stars.¹ Radial velocity measurements of all but one of them are consistent (within errors) with circular orbits; i.e., zero eccentricity (e.g., Laughlin et al. 2005). Presumably, any initial eccentricity in those orbits has since been damped by tidal circularization (Trilling 2000). In light of the discovery of the first transiting extrasolar planet with an eccentric orbit, HD 147506b, I explore the effect that orbital eccentricity has on transit light curves with an eye toward the data to come from *COROT* and *Kepler*.

Since tidal circularization is most effective at short planet-star distances, as transit search programs extend into longer period regimes, the prospects for detecting noncircularly orbiting planets grows. Perhaps not coincidentally, the first known transiting planet on an eccentric orbit, HD 147506b ($e = 0.507$), is the transiting planet with the longest period (5.63 days; Bakos et al. 2007). Recently, *Spitzer* measurements of the relative timing of the secondary eclipse of GJ436b have confirmed that planet's nonzero orbital eccentricity and measured it to be $e = 0.14 \pm 0.01$ (Demory et al. 2007).

With the space-based transit searches of *COROT* (Bordé et al. 2003) and particularly *Kepler* (Basri et al. 2005), hundreds of transiting planets will be found that will not have been tidally circularized. Based on the findings from radial velocity planet

searches (Butler et al. 2006), many of these newly discovered transiting planets are likely to follow eccentric orbits.

Orbital eccentricity has several effects on planetary transits. The timing of the transit, relative to that of the secondary eclipse, is a strong function of the planet's orbital eccentricity and longitude of periastron (e.g., Laughlin et al. 2005; Winn et al. 2007). Planets with eccentric orbits, if sufficiently close to their parent stars, can have their rotations brought into tidal equilibrium at rotation rates greater than their mean motions (Barnes & Fortney 2003); this affects planetary transit light curves via the planet's oblateness (Seager & Hui 2002; Barnes & Fortney 2003). These effects and others have been explored in the context of eclipsing binary stars on eccentric orbits as well (e.g., Nelson & Davis 1972).

In this paper, I explore three additional ways that orbital eccentricity affects the transits of extrasolar planets. First, I calculate the increased transit probability for planets on eccentric orbits. Next, I point out the variability in transit duration that results from planets moving faster near periastron and slower near apoastron. The third effect that I explore is the possibility of asymmetric transit light curves induced as the planet's trajectory evolves between transit ingress and egress. I then use least-squares fits of synthetic transit light curves to determine whether or not these effects can be used to constrain the orbital elements of transiting planets from photometry alone. Although orbital eccentricity is not inherent to the planet itself, I will sometimes refer to planets on eccentric orbits as "eccentric planets" for brevity, following (Lissauer et al. 1997).

¹ See listing online at <http://exoplanet.eu>.

2. EFFECTS

An extrasolar planet on an eccentric orbit has three primary differences relative to that same planet on a circular orbit with the same semimajor axis. The eccentric planet is more likely to transit, and if it does, then the transit duration depends on both the impact parameter b and the orbital true anomaly f , and the transit light curve may be asymmetric due to accelerations during the transit.

2.1. Transit Probability

Planets on eccentric orbits are more likely to transit than equivalent planets with the same semimajor axis but circular orbits. Although these planets spend a majority of their *time* at greater astero-centric distances than their semimajor axes, they spend a majority of their *true anomalies* at smaller astero-centric distances. The probability for a planet on a circular orbit to transit was derived by Borucki & Summers (1984) based on the solid angle swept out by a planet's shadow,

$$p = \frac{R_*}{r_p}, \quad (1)$$

where p is the transit probability, R_* is the stellar radius, and r_p is the distance between the planet and the star.

Using the method of Borucki & Summers (1984) then, the transit probability for an extrasolar planet is equal to the solid angle swept out by the planet's shadow, a function of both f and the polar angle from the orbit plane θ , normalized to 4π steradians,

$$p = \frac{1}{4\pi} \int_0^{2\pi} \int_{\theta_0}^{\theta_1} \cos \theta \, d\theta \, df, \quad (2)$$

using θ_0 and θ_1 for the angular extent of the shadow below and above the orbital plane. Because of the symmetry of the problem $\theta_0 = -\theta_1$. Geometry sets $\theta_1 = \sin^{-1}(R_*/r_p)$ (see Fig. 1). Hence, integrating over θ ,

$$p = \frac{1}{4\pi} \int_0^{2\pi} \sin \theta \Big|_{\theta_0}^{\theta_1} df, \quad (3)$$

and plugging in θ_0 and θ_1 ,

$$p = \frac{1}{4\pi} \int_0^{2\pi} \frac{2R_*}{r_p} df. \quad (4)$$

For planets on eccentric orbits, r_p varies with time. However, the variation of r_p as a function of f is all that matters for determining the solid angle over which the planet will transit

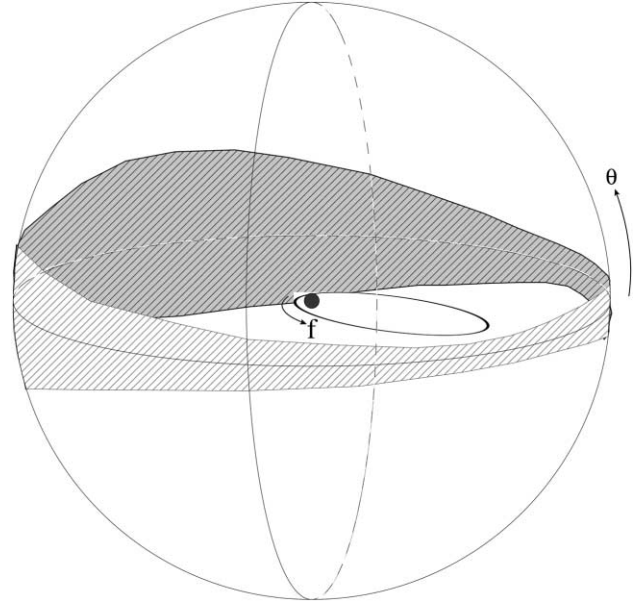


FIG. 1.—Geometry of an planetary orbit and the solid angle swept out by its shadow, modified from Borucki & Summers (1984) to account for orbital eccentricity.

(Murray & Dermott 2000),

$$r_p = \frac{a_p(1 - e^2)}{1 + e \cos f}, \quad (5)$$

where e is the planet's orbital eccentricity and a_p is its semimajor axis.

Plugging in r_p from equation (5) and integrating over f ,

$$p = \int_0^{2\pi} \frac{2R_*(1 + e \cos f)}{a_p(1 - e^2)} df \quad (6)$$

leads to

$$p = \frac{1}{4\pi} \frac{2R_*}{a_p(1 - e^2)} \int_0^{2\pi} 1 + e \cos(f) df, \quad (7)$$

which leads to the result that for planets on eccentric orbits,

$$p = \frac{R_*}{a_p(1 - e^2)}, \quad (8)$$

since $\int_0^{2\pi} df = 2\pi$ and $\int_0^{2\pi} \cos f df = 0$.

The above derivation is valid for transit impact parameters $b \leq 1$. To exclude all grazing transits, replace the R_* in the numerator of equation (8) with $R_* - R_p$, where R_p is the radius of the transiting planet. In a similar manner, to include all transits, no matter how grazing, the numerator of equation (8) would be $R_* + R_p$.

The increased transit probability for even a planet with a significantly eccentric orbit with $e = 0.5$, similar to that for HD 147506b (Bakos et al. 2007), is modest: 33%. However, the increased probability for planets on extremely eccentric orbits like HD 80606b (Naef et al. 2001) with $e = 0.93$ is 640%! Given that 28 of the 224 planets with radial velocity orbits have $e \geq 0.5$,² transit surveys should detect a significant number of planets on eccentric orbits. Nearly half, 110 out of 224, of radial velocity planets are more eccentric than our solar system's most eccentric planet, Mercury ($e = 0.2056$). Planets with extreme orbital eccentricities will be detected at a rate decidedly higher than their occurrence would predict given equation (1).

This excess will lead to a bias in the raw planet incidence as a function of semimajor axis derived from *COROT* and *Kepler* discoveries. The bias can be easily corrected by accounting for the $(1 - e^2)^{-1}$ detection increase factor from equation (8) or, more formally, by using the original Borucki & Summers (1984) probability (eq. [1]) while substituting the instantaneous planet–star distance at midtransit for the orbital radius for each detected planet.

Debiasing requires knowledge of the planet's orbital eccentricity and longitude of periapsis, which would be difficult to ascertain for planets too small to induce detectable radial velocity variations (§ 3). Although this extra step adds complexity, it is heartening to note that the orbital eccentricity bias induced in planet distributions as derived using the transit method is precisely calculable and removable. The orbital eccentricity bias in radial velocity planet surveys (as results from data gaps near periastron passage, for example) is known less precisely and is therefore more challenging to remove.

The differing transit probability at periastron and apoastron can lead to planets that transit, but have no secondary eclipse if the planet is sufficiently eccentric, inclined, and transits near periastron. Alternately, there can exist planets that show secondary eclipses but no primary transit. In the case in which giant planets have only secondary eclipses, the small secondary eclipse depth could be mistaken for the primary transit of a terrestrial-sized planet. Careful monitoring of reflected-light phase variability (as described in Jenkins 2002) may eliminate this source of systematic error. Secondary-eclipse-only planets would need to be very near their parent stars during secondary eclipse in order to have sufficient reflected light, so as to mimic the transit of a terrestrial-sized planet. Faint secondary stars in similar orbits could mimic the terrestrial planet transit regardless of their distance from the primary star at secondary eclipse.

2.2. Transit Duration

For a given star mass, planets with the same orbital semimajor axes have the same energy per unit mass ($-GM_*/2a_p$);

those with higher eccentricities have lower specific angular momenta. As such, those more highly eccentric objects move faster near periastron, and slower near apoastron. If such an eccentric planet were to transit, it would then have transits of shorter or longer duration than the equivalent planet on a circular orbit transiting with the same impact parameter (b).

The velocity of a circularly orbiting planet V_{circ} is

$$V_{\text{circ}} = \sqrt{\frac{GM_*}{a_p}}. \quad (9)$$

Using conservation of energy, the periapsis velocity V_{peri} of a planet with orbital eccentricity e can be shown to be

$$V_{\text{peri}} = \sqrt{\frac{1+e}{1-e}} \sqrt{\frac{GM_*}{a_p}} = \sqrt{\frac{1+e}{1-e}} V_{\text{circ}} = \sqrt{1+e} V_{\text{peri, circ}}. \quad (10)$$

In the case of planets discovered by their transits, a_p is set by the planet's known orbital period, and hence, the comparison to V_{circ} is most relevant. For convenience I also compare V_{peri} to $V_{\text{peri, circ}}$, the velocity of a planet orbiting circularly at the eccentric planet's periastron. Similarly, at apoapsis

$$V_{\text{apo}} = \sqrt{\frac{1-e}{1+e}} \sqrt{\frac{GM_*}{a_p}} = \sqrt{\frac{1-e}{1+e}} V_{\text{circ}} = \sqrt{1-e} V_{\text{apo, circ}} \quad (11)$$

for similarly named variables (see Fig. 2).

The pericenter and apocenter velocities behave as expected in their extremes. V_{peri} approaches escape velocity ($\sqrt{2}V_{\text{peri, circ}}$) as $e \rightarrow 1$ but is undefined for nonclosed orbits where $e \geq 1$. $V_{\text{apo}} \rightarrow 0$ as $e \rightarrow 1$, in absolute terms, as a function of V_{circ} , and as a function of $V_{\text{apo, circ}}$.

A significantly eccentric planet with $e = 0.5$ (similar to HD 147506b for which $e = 0.507$) travels $\sqrt{3}$ (~ 1.73) times faster at periapsis than you would expect, given its period and assuming a circular orbit, and $3^{-1/2}$ times as quickly at apoapsis. This planet's transit duration, if it were to transit at periastron, would be 58% as long for a particular impact parameter as the transit of its circularly orbiting equivalent. If transiting at apoastron (3 times less probable than a periastron transit; see § 2.1), the transit would last 73% longer than the equivalent circularly orbiting planet.

A planet on an extremely eccentric orbit like HD 80606b ($e = 0.93$; Naef et al. 2001) would have a periastron transit duration only 19% that of its same-semimajor-axis circular equivalent and 72% that of a planet orbiting circularly at HD 80606b's periastron. Conversely, if HD 80606b were to transit near apoastron, such a transit would last 5.25 times longer than

² See listing online at <http://exoplanet.eu>.

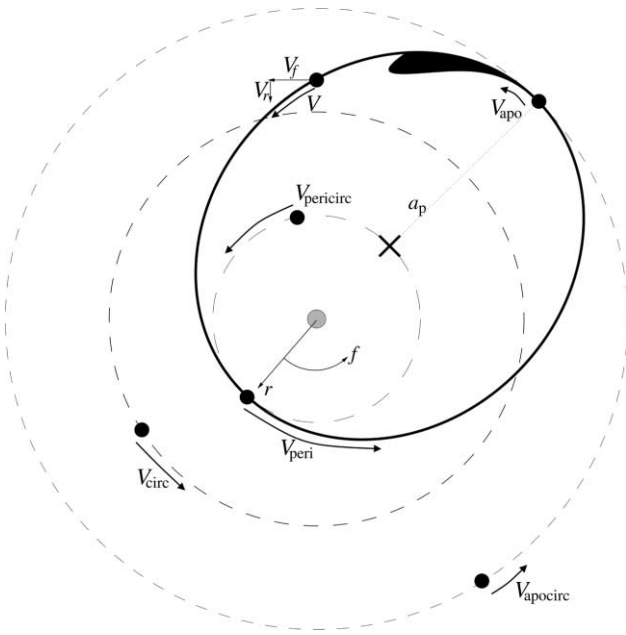


FIG. 2.—Variables described in § 2.2 of the text, as applied to a hypothetical planet with $e = 0.5$.

if HD 80606b were to transit in a circular orbit with the same semimajor axis and 3.78 times longer than if HD 80606b were to transit in a circular orbit at its true apoastron.

The duration of an exoplanetary transit depends on the chord length of the planet's apparent passage in front of the star ($2R_* \cos b$) and the planet's azimuthal velocity $V_f = rf$. In the cases discussed above, when a planet is at periastron and apoastron, V_{peri} and V_{apo} are equal to V_f . The rest of the time, V_f is not equal to the planet's full velocity, as the planet will also have a velocity component radial to the star (V_r). According to Murray & Dermott (2000) V_f varies sinusoidally with f ,

$$V_f = V_{\text{circ}} \frac{1 + e \cos f}{\sqrt{1 - e^2}}. \quad (12)$$

Hence, the planet's velocity is greater than the equivalent circular orbit velocity for more than half of the orbit as a function of the true anomaly.

2.3. Transit Symmetry

The dependence of the planet's azimuthal velocity on f as shown in equation (12) drives another effect that eccentric orbits have on transits. Because V_f changes slightly between ingress and egress (unless the planet is at periastron or apoastron midtransit), eccentric planets can produce asymmetric transit light curves. If a planet transits after periastron and before apoastron, the time that it takes for the planet to ingress across the star's limb will be shorter than the time that it takes to

egress. Similarly, if the planet is between apoastron and periastron, then the ingress will be longer than the egress.

To calculate the velocity difference between ingress and egress, I first take V_f from equation (12) and differentiate it with respect to f ,

$$\frac{dV_f}{df} = -\frac{eV_{\text{circ}}}{\sqrt{1 - e^2}} \sin f. \quad (13)$$

The total ingress-egress velocity difference ΔV is equal to dV_f/df times Δf , the difference of the true anomaly between ingress and egress, under the assumption that dV_f/df varies negligibly across the transit. Taking f_0 to be the true anomaly of the planet at midtransit,

$$\Delta f = \frac{2R_*}{r_p(f_0)}, \quad (14)$$

assuming that r_p varies only slowly during the transit. Now, plugging in r_p from equation (5),

$$\Delta V = \frac{dV_f}{df} \Delta f = -\frac{2R_* e V_{\text{circ}}}{a(1 - e^2)^{3/2}} \sin f_0 (1 + e \cos f_0). \quad (15)$$

I show a plot of the varying component of ΔV for various values of e in Figure 3. The *fractional* difference in velocity, $\Delta V/V$, is a bit simpler,

$$\frac{\Delta V}{V} = -\frac{2R_* e}{a(1 - e^2)} \sin f_0, \quad (16)$$

and has an evident maximum where $f_0 = \pm\pi/2$. Hence, the greatest *fractional* variation in ingress and egress duration will occur 90° away from periastron and apoastron, as measured in the planet's true anomaly.

To determine where the *absolute* velocity difference ΔV is maximized, I differentiate ΔV with respect to f and set the result equal to zero,

$$0 = \frac{d\Delta V}{df} = -\frac{2R_* e V_{\text{circ}}}{a(1 - e^2)^{3/2}} \frac{d[\sin f_0 + e \sin f_0 \cos f_0]}{df}. \quad (17)$$

Differentiating and using the double-angle formula $\sin(2x) = 2 \sin x \cos x$, I determine that

$$\cos f_0 + e \cos(2f_0) = 0. \quad (18)$$

I show the solution to this equation in Figure 4. The maximum velocity difference occurs at $f_0 = \pm\pi/2$ for infinitesimal eccentricities and approaches $f_0 = \pm\pi/3$ as $e \rightarrow 1$.

To illustrate the consequences of this effect, I apply the results derived above to newly discovered eccentric transiting

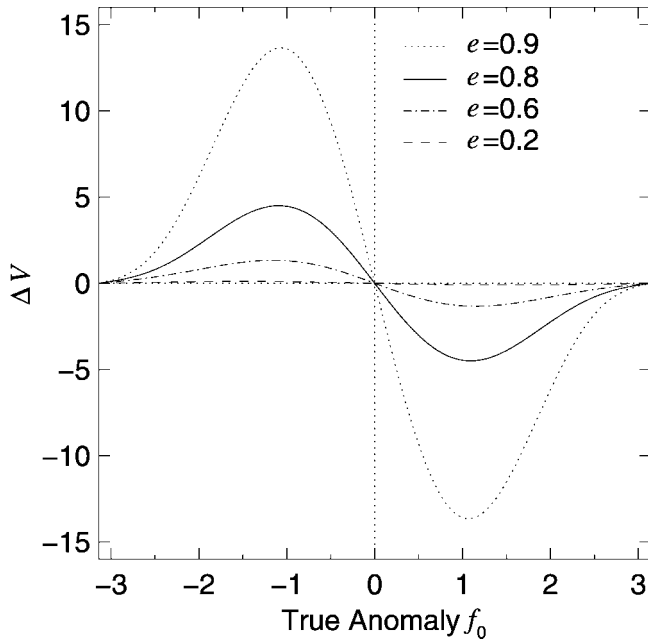


FIG. 3.—Velocity difference between egress and ingress as a function of the planet’s orbital true anomaly at midtransit f_0 . I have only plotted that portion of eq. (15) that is a function of f and e ; to convert to true ΔV , multiply by $2R_* V_{\text{circ}}/a$. As an example, the multiplier for a planet in an $a_p = 0.1$ AU orbit around a $1 M_\odot$ star is 8.76 km s^{-1} .

planet HD 147506b (Bakos et al. 2007). HD 147506b was determined by its discoverers (Bakos et al. 2007) to have a radius of $1.18 R_{\text{Jup}}$, an orbital semimajor axis of 0.0685 AU, an orbital eccentricity of 0.507, and a longitude of periastron of 184.6° . The planet’s parent star, HD 147506, was determined to have a radius of $1.8 R_\odot$ and a mass of $1.35 M_\odot$ (note that refined system parameters were published by Loeillet et al. [2007] while this paper was in review; the new values do not change the qualitative results that I describe here, but future work should employ these newer values). I show a to-scale schematic of the system in Figure 5.

From equation (12) HD 147506b’s V_{circ} is 132.2 km s^{-1} . This planet’s orbital parameters are particularly favorable with respect to maximizing the magnitude of ΔV_f . HD 147506b’s large eccentricity, fast V_{circ} , and nearly ideal true anomaly at midtransit ($f_0 = 4.84$, very close to $-\pi/2$), combined with HD 147506’s large stellar radius, yield $\Delta V_f = -24.6 \text{ km s}^{-1}$. Calculating the ingress and egress times τ using

$$\tau = \frac{R_p}{V_f \cos(\sin^{-1} b)} \quad (19)$$

with the appropriate V_f values for the transit ingress and egress of HD 147506b yields $\tau_{\text{ingress}} = 10 \text{ minutes } 36 \text{ s}$ and $\tau_{\text{egress}} = 8 \text{ minutes } 37 \text{ s}$.

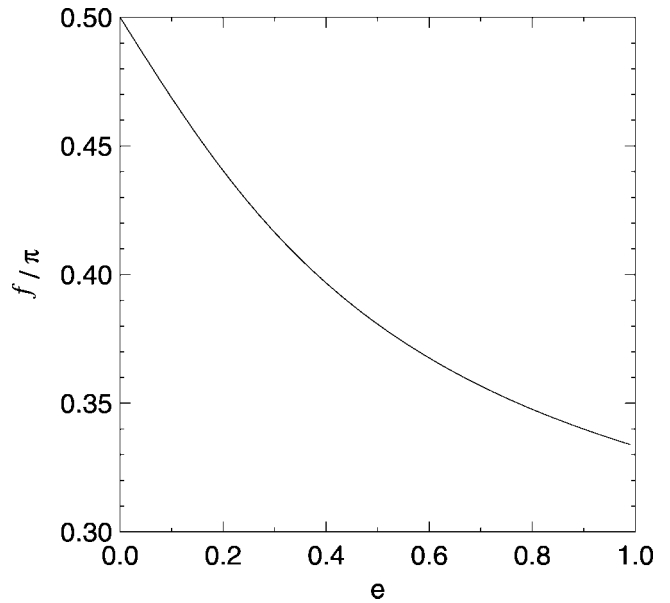


FIG. 4.—True anomaly at midtransit (f_0 ; here in units of radians divided by π) for which the difference between a planet’s transit ingress and egress velocity is maximized as a function of the planet’s orbital eccentricity e .

3. DETECTABILITY

The *COROT* and *Kepler* missions will discover hundreds of new transiting extrasolar planets (Bordé et al. 2003; Basri et al. 2005). The most massive of these will be amenable to radial

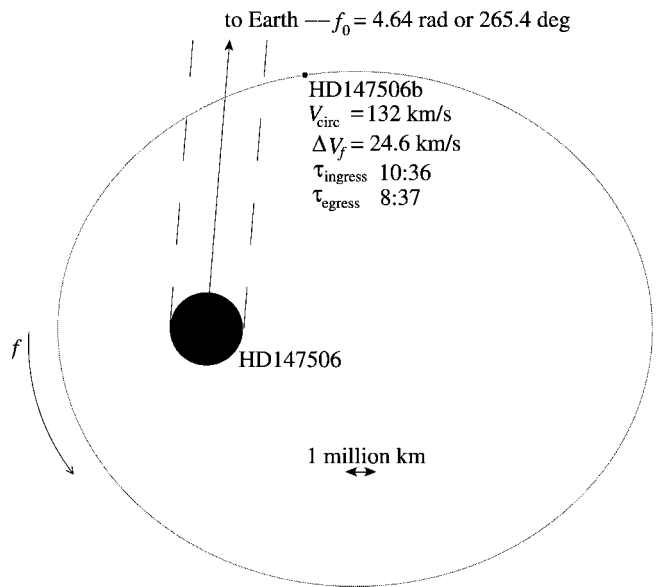


FIG. 5.—To-scale diagram of the HD 147506 system. Ingress and egress times listed are in minutes : seconds format. Figure concept inspired by G. Laughlin’s Web site (at <http://oklo.org>).

velocity follow-up observations to measure their masses; a more complete set of radial velocity measurements (i.e., covering the full orbit and not just the radial velocity maxima and minima, which are all that would be required to determine mass assuming a circular orbit and the epoch and period as established by the transit) can determine the planets' orbital eccentricities and longitudes of periastron. However, for planets of Neptune mass and smaller, in larger orbits, or orbiting fainter stars, radial velocity follow-up will not be practical or in some cases possible. In those cases, it would be useful to attempt to constrain the orbital eccentricity of those planets using transit photometry alone. Such a determination would bear critically on the climatic variability of Earth-like worlds; highly eccentric planets may not be habitable even if their orbital semimajor axes place them within their stars' habitable zone.

To determine the photometric detectability of the transit duration and asymmetry effects of eccentric planet orbits, I create synthetic transit light curves that I then fit as if the orbit were circular. I assume knowledge of the planet's period, as that value will be measured by the time between transits in *Kepler* and *COROT* data. I calculate both the synthetic light curves and the best-fit solutions using the analytical approximation of Mandel & Agol (2002). The Mandel & Agol (2002) formulation assumes that the portion of the star covered by the planet has uniform surface brightness, but that brightness accounts for limb darkening; hence, it is least accurate for ingress and egress. However, the detrimental effects on this particular calculation should be minimal, since both the synthetic and best-fit light curves should show the same systematic errors, which, when subtracted, should leave a good estimate for the proper fit residuals. The effects of light-travel delay illustrated by Loeb (2005) are not included.

For larger planets, those where the ingress and egress are temporally resolved, that have high signal-to-noise ratio light curves, I first fit for R_* , R_p , the transit impact parameter b , and a stellar limb-darkening coefficient c_1 , the treatment applied to HD 209458b by Brown et al. (2001). I assume a $1 R_{\text{Jup}}$ planet orbiting a $1 R_{\odot}$, $1 M_{\odot}$ star with $a_p = 0.1$ AU and $e = 0.5$. Since R_p/R_* is set by the transit depth and b by the ingress/egress time relative to the total transit duration, orbital eccentricity in this type of fit systematically affects R_* , which governs the total transit timescale. In my test runs, the best-fit $R_{*,\text{measured}}$ varies as $R_{*,\text{measured}} = R_* V_{\text{circ}} V_{f_0}^{-1}$. Hence, assuming a circular orbit when the orbit is actually eccentric leads to a systematic error in the measurement of R_* and, by extension, R_p (R_p/R_* is unaffected). The measured values are smaller than the actual values if the planet is near periastron and are larger if the planet is near apoastron.

This systematic error can be addressed by assuming a stellar radius, as could be estimated by other observations such as parallax, spectral type, and stellar absolute magnitude. In this case, the transit timescale can be set by fitting explicitly for V_{f_0} in addition to r_p , b , and c_1 . However, without knowledge of

the midtransit true anomaly f_0 , V_{f_0} cannot uniquely determine the orbital eccentricity. Instead, V_{f_0} can *constrain* e if we allow that the planet must have a minimum eccentricity in order that V_f reach V_{f_0} . If $V_{f_0} > V_{\text{circ}}$, then from equation (10),

$$e \geq \frac{(V_{f_0}/V_{\text{circ}})^2 - 1}{(V_{f_0}/V_{\text{circ}})^2 + 1}, \quad (20)$$

and if $V_{f_0} < V_{\text{circ}}$, then similarly from equation (11),

$$e \geq \frac{1 - (V_{f_0}/V_{\text{circ}})^2}{1 + (V_{f_0}/V_{\text{circ}})^2}. \quad (21)$$

The above lower limits can only be placed when the planet's ingress and egress are resolved. In order to constrain the eccentricity of terrestrial-sized planets, both high temporal cadence and high photometric precision would be necessary. Resolving the ingress of the Earth, with $\tau_{\text{ingress}} = 7.04$ minutes at $b = 0$, will not be possible given *Kepler* data alone. Co-addition of multiple transits from multiple telescopes might help to constrain the ingress times for detected transiting terrestrial planets.

The degeneracy between e and f_0 , multiple combinations of which can produce the same V_{f_0} , can be broken by measuring the transit asymmetry outlined in § 2.3. To measure the detectability of the asymmetry, I produce a synthetic light curve for HD 147506b ($r_p = 1.18 R_{\text{Jup}}$, $R_* = 1.8 R_{\odot}$, $a_p = 0.0685$ AU, $e = 0.507$, $f_0 = 4.84$, and assuming the Brown et al. [2001] limb-darkening coefficient $c_1 = 0.64$) that I fit using a model planet with a circular orbit. The residuals, which I refer to as the detectability, are shown in Figure 6 for transits at several impact parameters.

When faced with an ingress and egress of differing duration, the best-fit circular-orbit planet model splits the difference. On ingress for HD 147506b, which transits before periastron ($f_0 = -1.44$), the real planet is moving more slowly than the model planet. In the difference light curve, the real planet hits the stellar limb *before* the model, such that at mid-ingress the real and model planets are in the same place. So the real-minus-model detectability initially trends negative, reaches zero at mid-ingress, and then trends positive until the end of the planet's ingress. The detectability varies slowly between the end of ingress and the beginning of egress, resulting from the planet covering stellar areas that have been slightly differently limb darkened.

The process is reversed on egress. With the planet now moving more quickly than the circular-orbit model, the model begins its egress early, so that the real planet will have caught up with it by mid-egress. Hence, the real-minus-model detectability is again initially negative, reaches zero by mid-egress, and then trends positive until the end of egress for both the real and model planets.

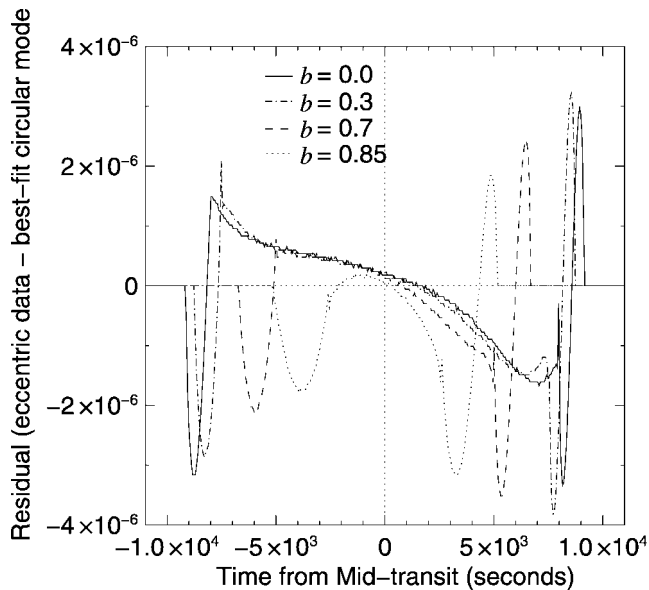


FIG. 6.—Detectability of the transit light curve asymmetry induced by the orbital eccentricity of planet HD 147506b, for impact parameters $b = 0.0, 0.3, 0.7,$ and 0.85 .

Despite the large ΔV for HD 147506b, the magnitude of the transit light curve asymmetry induced by orbital eccentricity is rather low (Fig. 6), peaking at only 3×10^{-6} of the stellar flux. This low detectability is unmeasurable given current capabilities and will probably prove challenging in the future as well given inherent stellar variability. The large stellar radius of HD 147506 increases ΔV but also decreases R_p/R_* , diminishing the asymmetry effect. Hence, although measurement of the asymmetry induced by an eccentric planet orbit can, along with V_j , uniquely determine both e and the longitude of periastron, the small magnitude and duration of the effect are such that a measurement is unlikely to be practical.

For transiting terrestrial-sized planets, determination of orbital eccentricity is even more difficult. If the ingress and egress are temporally resolved, that duration along with the total transit duration together set the transit impact parameter and V_j , providing a minimum e constraint as per equations (20) and (21). For objects with such small transit depths as terrestrial planets, however, it will be difficult to temporally resolve the planets' ingress and egress.

Another way to constrain b for terrestrial planets would be to use the effect of stellar limb darkening. Seager & Mallén-Ornelas (2003) showed that minimizing limb darkening more precisely delineates the end of a planet's ingress and the beginning of its egress. However, strong limb darkening, if well-understood, can provide a mechanism for ascertaining a transit's impact parameter. Similar to the analysis used by Knutson et al. (2007) to study HD 209458b, fixing limb-darkening coefficients based on theoretical or previously determined values could suffice in constraining b , which, with a previously mea-

sured R_* , would then determine V_j and allow constraints to be placed on e .

4. CONCLUSIONS

For a given orbital semimajor axis, extrasolar planets on eccentric orbits are more likely to transit than planets on circular orbits by a factor of $(1 - e^2)^{-1}$. As the space-based transit surveys *COROT* and *Kepler* discover transiting planets that are far enough from their parent stars to have avoided tidal circularization, more highly eccentric planets will be found preferentially. This bias is easy to remove if the eccentricity and longitude of periastron are known, as they could be given follow-up radial velocity observations.

The duration of a transit is a function of the planet's tangential velocity at midtransit V_{j0} . For eccentric planets V_{j0} is greatest at periastron and smallest at apoastron. Hence, if a planet transits near periastron, the duration is shorter than that of an equivalent planet in a circular orbit, and likewise, transits that occur when a planet is near apoastron are longer than those of the equivalent circularly orbiting planet. It would be useful to be able to use this effect to determine the orbital eccentricity of discovered transiting extrasolar planets, either before or without radial velocity follow-up.

If fitting the resulting light curve with a model planet on a circular orbit with the known planetary period, a systematic error results in the determination of the transit parameters if fitting for R_* , R_p , b , and c_1 , as done by Brown et al. (2001) for HD 209458b. If instead the model system uses an assumed stellar radius measured by different means, then the transit velocity V_{j0} can be measured. However, without another, independent measurement of either e or the planet's longitude of periastron, knowledge of V_{j0} cannot alone determine those parameters. It can set a lower limit on a planet's orbital eccentricity.

The difference in V_j between a planet's ingress and egress that results from the planet's orbital accelerations can resolve the e /longitude of periastron degeneracy. This velocity differential ΔV introduces an asymmetry into the transit light curve; ingress is longer than egress before periastron, and shorter after periastron. My model fits to synthetic eccentric planet transit light curves show that the detectability of this asymmetry is small, of order 3×10^{-6} for the recently discovered eccentric transiting planet HD 147506b. An effect that small is undetectable using present techniques. As HD 147506b is nearly a model candidate for observing this effect, it is unlikely that transit light curve asymmetry will prove useful for determining the orbital parameters of transiting planets using photometry alone.

Determination of orbital eccentricity is of critical importance for evaluating the habitability of terrestrial-sized transiting planets discovered by *Kepler*. As these planets have masses too low for radial velocity measurements to detect, our only constraints on e for these planets will be photometric. If the

stellar radius can be assumed from other prior measurements, then it is possible to use theoretical stellar limb-darkening coefficients within the *Kepler* bandpass to measure the transit impact parameter. This measurement would then constrain V_{f_0} and allow a lower limit to be placed on e .

No techniques currently available will be able to uniquely measure the orbital eccentricity of the terrestrial extrasolar planets that *Kepler* will discover. The lower limits on eccentricity described above will allow for a statistical exploration of the eccentricity distribution of terrestrial planets. That distribution

will serve to constrain the formation and evolution of such planets, as it has done for giant planets. However, whether or not any particular *Kepler* planet is truly habitable will remain unknown until its orbital eccentricity can be measured.

J. W. B. acknowledges the support of the NASA Postdoctoral Program, administered for NASA by Oak Ridge Associated Universities and the support of NASA's *Kepler* mission for publication costs.

REFERENCES

- Bakos, G. A., et al. 2007, ApJ, submitted (arXiv:0705.0126v2)
 Barnes, J. W., & Fortney, J. J. 2003, ApJ, 588, 545
 Basri, G., Borucki, W. J., & Koch, D. 2005, NewA Rev., 49, 478
 Bordé, P., Rouan, D., & Léger, A. 2003, A&A, 405, 1137
 Borucki, W. J., & Summers, A. L. 1984, Icarus, 58, 121
 Brown, T. M., Charbonneau, D., Gilliland, R. L., Noyes, R. W., & Burrows, A. 2001, ApJ, 552, 699
 Butler, R. P., et al. 2006, ApJ, 646, 505
 Demory, B. et al. 2007, A&A, submitted (arXiv:0707.3809v2)
 Jenkins, J. M. 2002, ApJ, 575, 493
 Knutson, H. A., Charbonneau, D., Noyes, R. W., Brown, T. M., & Gilliland, R. L. 2007, ApJ, 655, 564
 Laughlin, G., Marcy, G. W., Vogt, S. S., Fischer, D. A., & Butler, R. P. 2005, ApJ, 629, L121
 Lissauer, J. J., Berman, A. F., Greenzweig, Y., & Kary, D. M. 1997, Icarus, 127, 65
 Loeb, A. 2005, ApJ, 623, L45
 Loeillet, B., et al. 2007, A&A, submitted (arXiv:0707.0679v1)
 Mandel, K., & Agol, E. 2002, ApJ, 580, L171
 Murray, C. D., & Dermott, S. F. 2000, Solar System Dynamics (New York: Cambridge Univ. Press)
 Naef, D., et al. 2001, A&A, 375, L27
 Nelson, B., & Davis, W. D. 1972, ApJ, 174, 617
 Seager, S., & Hui, L. 2002, ApJ, 574, 1004
 Seager, S., & Mallén-Ornelas, G. 2003, ApJ, 585, 1038
 Trilling, D. E. 2000, ApJ, 537, L61
 Winn, J. N., et al. 2007, AJ, 133, 1828